

A simple route to a tunable electromagnetic gateway

To cite this article: Huanyang Chen *et al* 2009 *New J. Phys.* **11** 083012

View the [article online](#) for updates and enhancements.

Related content

- [Topical Review](#)
Huanyang Chen and C T Chan
- [Manipulating sources using transformation optics with folded geometry](#)
Yun Lai, Huihuo Zheng, Zhao-Qing Zhang *et al.*
- [Shrinking optical devices](#)
W H Wee and J B Pendry

Recent citations

- [Invisible gateway for both light waves and rays](#)
Fei Sun and Sailing He
- [Optical illusions induced by rotating medium](#)
XiaoFei Zang *et al*
- [Polarization properties of defect mode in one-dimensional magnetic photonic crystal](#)
Guangbin Wu *et al*

A simple route to a tunable electromagnetic gateway

Huanyang Chen¹, Che Ting Chan^{1,3}, Shiyang Liu²
and Zhifang Lin²

¹ Department of Physics and the William Mong Institute of NanoScience and Technology, The Hong Kong University of Science and Technology, Clear Water Bay, Hong Kong, People's Republic of China

² Surface Physics Laboratory, Department of Physics, Fudan University, Shanghai 200433, People's Republic of China

E-mail: phchan@ust.hk

New Journal of Physics **11** (2009) 083012 (13pp)

Received 6 May 2009

Published 13 August 2009

Online at <http://www.njp.org/>

doi:10.1088/1367-2630/11/8/083012

Abstract. Transformation optics is used to design a gateway that can block electromagnetic waves but allows the passage of other entities. Our conceptual device has the advantage that it can be realized with simple materials and structural parameters and can have a reasonably wide bandwidth. In particular, we show that our system can be implemented by using a magnetic photonic crystal structure that employs a square array of ferrite rods, and as the field response of ferrites can be tuned by external magnetic fields, we end up with an electromagnetic gateway that can be open or shut using external fields. The functionality is also robust against the positional disorder of the rods that make up the photonic crystal.

³ Author to whom any correspondence should be addressed.

Contents

1. Introduction	2
2. A new ‘superscatterer’	2
3. An invisible electromagnetic gateway	4
4. The implementation of a tunable electromagnetic gateway	7
5. Conclusion	9
Acknowledgments	9
Appendix A	9
Appendix B	11
References	12

1. Introduction

Transformation optics [1]–[3] has paved the way for the development of optical devices that can realize functionalities that were thought to be possible only in science fiction [4]–[18]. Luo *et al* [19] have recently proposed a conceptual device that has attracted great public interest. This device is a gateway that can block electromagnetic waves but that allows the passage of other entities. It can be viewed as an implementation of a ‘hidden portal’ mentioned in fiction [20]. However, the feasibility of such devices is limited by the very complex material parameters and the narrow bandwidth. Here, we show that gateway-type devices can actually be realized with simple parameters and they can have wider bandwidths such that the concept is closer to reality [21]–[26] than previously thought. The structure can be implemented by using magnetic photonic crystal structures that are field tunable, resulting in an invisible electromagnetic gateway that can be open or shut using magnetic fields.

2. A new ‘superscatterer’

We start from a simple implementation of transformation optics. In figure 1(a), an object (colored in blue) is placed to the left side of a double negative medium (DNM) with $\varepsilon = \mu = -1$. Let the object be of permittivity ε_0 and permeability μ_0 . The detailed shape and the length scale of the structure are shown in figure 1(a). From the viewpoint of transformation optics, the whole structure is optically equivalent to another object described in figure 1(b) for far-field observers. The equivalent permittivity and permeability tensors are $\vec{\varepsilon} = \varepsilon_0 \vec{c}$ and $\vec{\mu} = \mu_0 \vec{c}$ with a constant tensor \vec{c} . We introduce some parameters for ease of reference following the coordinates x_1, x_2, y_1, y_2 and the angle α in figure 1. Let $\Delta = x_2 - x_1$ be the waist of the object in the x -direction, $r = \frac{\Delta}{2x_1 + \Delta}$ be a coordinate compression ratio and

$$p = \begin{cases} \frac{1}{\tan \alpha} \frac{2(x_1 + \Delta)}{2x_1 + \Delta}, & y_1 < y < y_2, & -x_2 \frac{y_2 - y}{y_2 - y_1} < x < x_1 \frac{y_2 - y}{y_2 - y_1}, \\ 0, & |y| < y_1, & -x_2 < x < x_1, \\ -\frac{1}{\tan \alpha} \frac{2(x_1 + \Delta)}{2x_1 + \Delta}, & -y_2 < y < -y_1, & -x_2 \frac{y_2 + y}{y_2 - y_1} < x < x_1 \frac{y_2 + y}{y_2 - y_1}, \end{cases} \quad (1)$$

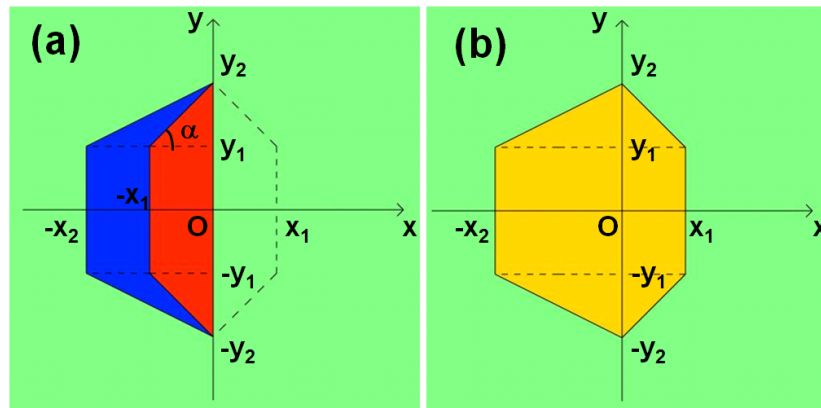


Figure 1. A simple electromagnetic structure comprising of two homogeneous regions (left panel) and an equivalent structure that gives the same scattering (right panel). (a) The schematic plot for the scatterer that appears electromagnetically larger than its physical size. The red region is the DNM, the blue region is the original isotropic material that is to the left of the DNM, and the green region represents the air background. x_1, x_2, y_1, y_2 and α are the detailed coordinates of the structure. The dashed lines in the region ($x > 0$) give the virtual boundary for the equivalent transformation medium. (b) The equivalent transformation medium is indicated by the yellow region, whose parameters are implemented by equation (2). The dashed lines distinguish the three different regions for the definition of p .

where (x, y) are the position coordinates of the equivalent transformation medium in figure 1(b). The inequalities for the definition of the parameter p come from three different coordinate transformations and the three regions are distinguished by the two dashed lines in figure 1(b).

It can be proved that (see appendix A):

$$\vec{c} = \begin{bmatrix} \frac{1+p^2}{r} & -p & 0 \\ -p & r & 0 \\ 0 & 0 & r \end{bmatrix}. \quad (2)$$

The coordinate transformation is based on the recent work on transformation optics with complementary media (or folded geometries) [27, 28]. The original object is mapped into the equivalent transformation medium. The DNM together with its mirror image (the boundary is marked by the dashed line in figure 1(a)) of air form a pair of complementary media, in the sense that the phase accumulated in one segment is exactly canceled by another. A more detailed discussion of the optical properties of this specific geometry and the associated coordinate transformation can be found in appendix A. The structure in figure 1(a) can be treated as a form of a scattering amplifier [29] because its scattering cross section can be much larger than its geometric cross section. The amplification effect originates from the excitation of surface plasmons in the DNM and air interface.

As a concrete example, we suppose that the original isotropic material (the blue region in figure 1(a)) has a large value of permittivity, $\epsilon_0 = -10\,000$ and $\mu_0 = 1$, which may be treated

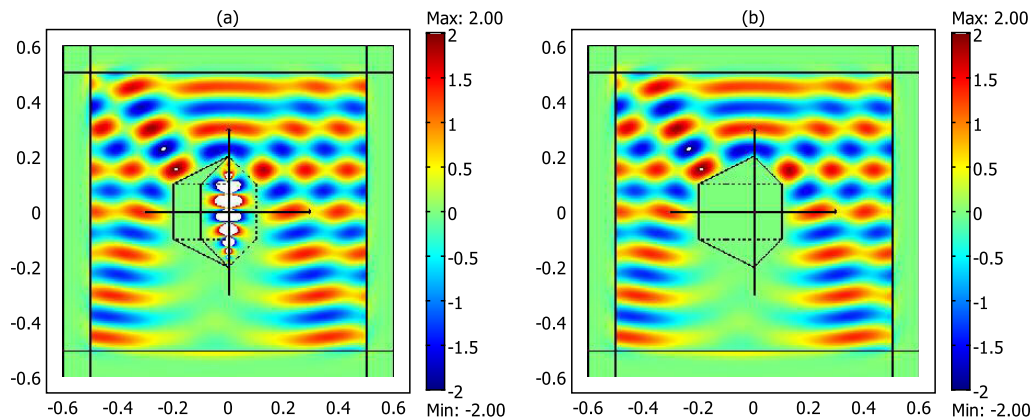


Figure 2. The scattering pattern for the scattering object and the equivalent scatterer. (a) The scattering pattern of the structure depicted in figure 1(a). (b) The scattering pattern of the equivalent material but with the PEC replacing the material implemented by equation (2).

approximately as a perfect electric conductor (PEC). Figure 2(a) shows the scattering field pattern of the structure in figure 1(a). The plane wave is incident from the top to the bottom and has transverse electric (TE) polarization, for which the E field is along the z -direction. In this paper, we only consider the TE modes for simplicity. Note that the same idea works for transverse magnetic (TM) modes as well. The frequency is 2 GHz and $x_1 = y_1 = 0.1$ m, $x_2 = y_2 = 0.2$ m and $\alpha = \pi/4$. The structure behaves like an equivalent material with parameters described by equation (2) to the far-field observers. Due to the large mismatch of the impedance of the equivalent material with the air background, we expect that the equivalent object (the yellow domain in figure 1(b)) should scatter like a PEC, and for that reason we choose for comparison in figure 2(b) the scattering field pattern of a perfect conductor filling up the entire domain of the virtual object in figure 1(b). The similar far-field scattered patterns between figures 2(a) and (b) confirm the strong scattering effect. The permittivity and permeability of the DNM are actually chosen as $-1 + 0.0001 \times i$ in the simulations to avoid numerical divergence problems [28]. The PEC-like scatterers are always chosen as materials of permittivity $-10\,000$ and the permeability is taken to be 1 in this paper for simplicity.

3. An invisible electromagnetic gateway

The amplified scattering effect can be utilized to make an invisible gateway [19]. Suppose that a PEC wall separates the whole space into two regions, the upper domain and the lower domain. If there are channels (or gateways) opened in the PEC wall, people in the two different spaces can communicate with each other, both physically and through electromagnetic (EM) waves. However, if we replace the doors with the above-described configuration at a specific frequency, the communication for that frequency will be blocked because the systems behave like PECs. The most amazing fact is that the channel is in fact physically empty. There is nothing but air in the channel so objects can ‘walk through’ but the channel is blocked as perceived by the eye because light at the designated frequency cannot penetrate. Figure 3 is a schematic plot of such a gateway based on the above idea. With the same scale as the one in figure 2(a), we demonstrate

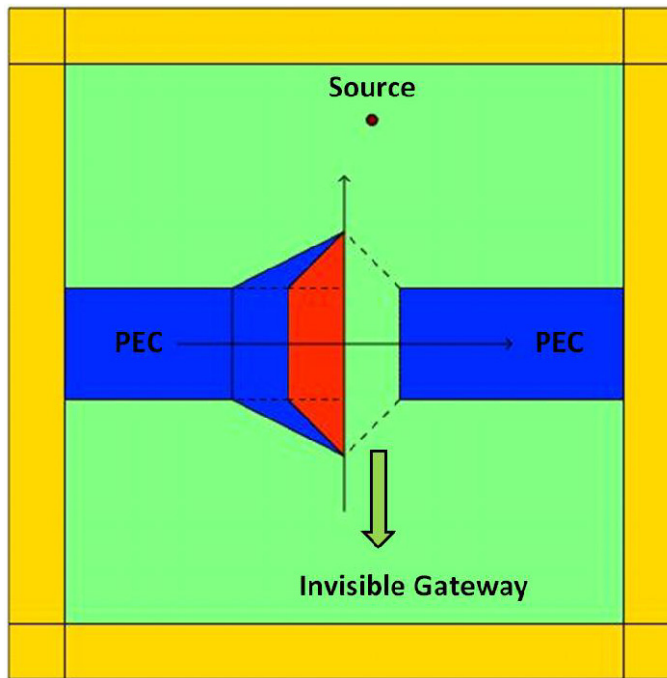


Figure 3. The computation domains for the electromagnetic gateway. The yellow regions are the perfectly matched layers (PMLs), the red region is the DNM, the green region is air, and the blue regions are PECs. The point source is located at above the gateway and it is denoted by a brown circle. The region between the DNM and the right PEC is the so-called ‘invisible gateway’.

the properties of such a gateway. We suppose that there is a line source located at (0.05 m, 0.4 m) with a frequency of 2 GHz in the upper domain. Figure 4(a) shows that the waves cannot pass through the gateway and are excluded from the lower domain. However, without the DNM, the waves can propagate into the lower region as shown in figure 4(b).

We now consider the bandwidth of such a device. To be more concrete, we consider the following dispersions for the DNM:

$$\begin{aligned}\varepsilon &= 1 - \frac{f_p^2}{f(f + i\Gamma)}, \\ \mu &= 1 - \frac{Ff^2}{f^2 - f_0^2 + i\gamma f},\end{aligned}\tag{3}$$

where $f_p = 2.828$ GHz, $\Gamma = 0.1$ MHz, $F = 1.5$, $f_0 = 1$ GHz and $\gamma = 0.075$ MHz. When $f = 2$ GHz, the relative permittivity and permeability return to $-1 + 0.0001 \times i$ used in the above simulations. When $f = 1.6$ GHz, the impedances do not match at the interface of air and the DNM, while the refractive index of the DNM is about -1.76 . Figure 4(c) shows the electric field pattern, whereas figure 4(d) shows the field without the DNM. The DNM can reduce the penetration of the waves from the upper region when compared with figures 4(c) and (d). However, as $n < -1$, there is still a ‘slit’ between the virtual boundary and the right PEC, which allows the waves to propagate somewhat into the lower region. If $n = -1$, the virtual

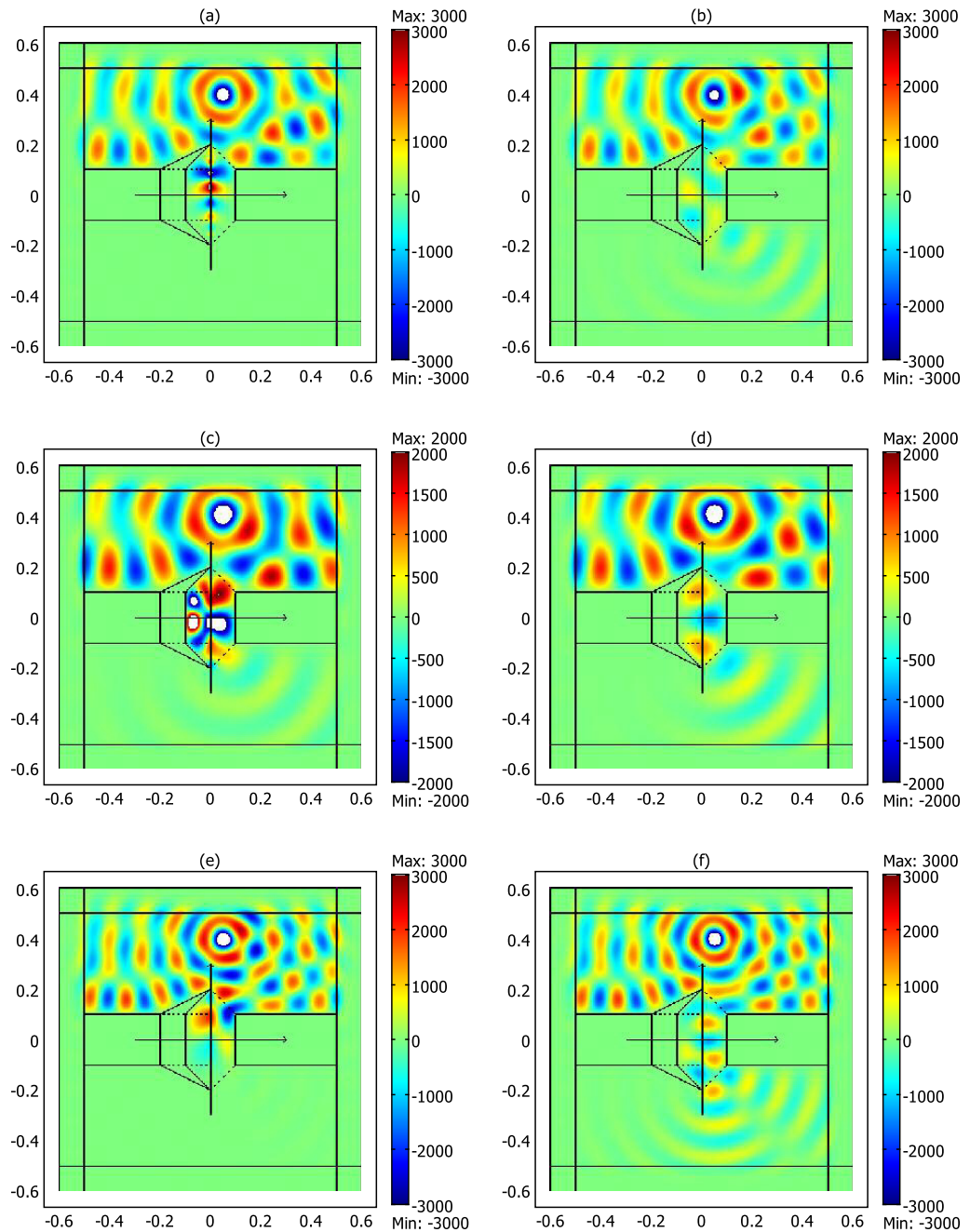


Figure 4. The functionalities of the gateway (with or without the DNM) at different frequencies. (a) The electric field pattern for the gateway at 2 GHz. (b) The electric field pattern for the gateway without the DNM at 2 GHz. (c) Same as (a) but for 1.6 GHz. (d) Same as (b) but for 1.6 GHz. (e) Same as (a) but for 2.4 GHz. (f) Same as (b) but for 2.4 GHz.

boundary is simply the mirror of the interface of the DNM and PEC on the left with $x = 0$ as the mirror. The position of the virtual boundary can be obtained heuristically from the image-forming principle. When $f = 2.4$ GHz, the impedances are still mismatched while the refractive index of the DNM is about -0.56 . As the absolute value of n decreases, the virtual boundary of the image expands and there will be no passage for the waves to penetrate because the virtual boundary overlaps with the PEC on the right-band side. For example, we plot the electric field pattern in figure 4(e) and the case without the DNM in figure 4(f). We find that the DNM can eliminate the penetration of the waves from the upper region. That means that the negative band of the DNM beyond $f = 2$ GHz (or $-1 < n < 0$) is the working frequency of the designed gateway. However, we also find that the wave blocking effect will become weaker with higher frequencies (in this case, about 2.5 GHz) in our simulations. As negative index media are intrinsically dispersive, the bandwidth has to be finite as the parameters will deviate progressively from those required by transformation optics. But the present gateway is shown to be relatively robust and has a broad operation bandwidth of about 20%, which can be regarded as a broadband device. To have a broader bandwidth, we can simply reduce the distance of the DNM and the right PEC to enhance the overlapping while the functionality of the gateway is sacrificed. As there are extensive designs of the DNMs at various wavelengths (both theoretically and experimentally) [21]–[26], it would be reasonably feasible for the present gateway to be realized in the future.

For higher frequencies, the working bandwidth will become narrow again like the situation described in [19]. Since the functionality of the invisible gateway comes from the evanescent waves in the DNM interface, the effect will disappear if we employ a geometric optics description. If the losses of the metamaterial are large (i.e. the imaginary parts of the parameters of the DNM are larger than 0.1), the bandwidth of the gateway will be small and the functionality will be compromised. The absorption of the DNM is the key difficulty for the gateway described here as for other devices such as the perfect lens. All our simulation results are calculated using the COMSOL Multiphysics finite element-based electromagnetics solver.

4. The implementation of a tunable electromagnetic gateway

Very recently, it has been demonstrated that the DNM can be realized with a simple array of ferrite rods without any metallic components [30], which can be used to implement the present gateway. One of the unique merits of this magnetic metamaterial is that its optical properties are magnetically tunable. As such, the gateway can be manipulated using external magnetic fields. The magnetic metamaterial is a periodic square array of subwavelength ferrite rods with radii of $r = 3.5$ mm and a lattice constant of $a = 10$ mm. The permittivity is taken to be $\epsilon = 25$, and the permeability of the ferrite rods has the form

$$\hat{\mu} = \begin{pmatrix} \mu_r & -i\mu_\kappa & 0 \\ i\mu_\kappa & \mu_r & 0 \\ 0 & 0 & 1 \end{pmatrix} \quad \text{with } \mu_r = 1 + \frac{\omega_m(\omega_0 - 2\pi i\alpha_1 f)}{(\omega_0 - 2\pi i\alpha_1 f)^2 - 4\pi^2 f^2}$$

and

$$\mu_\kappa = \frac{2\pi\omega_m f}{(\omega_0 - 2\pi i\alpha_1 f)^2 - 4\pi^2 f^2},$$

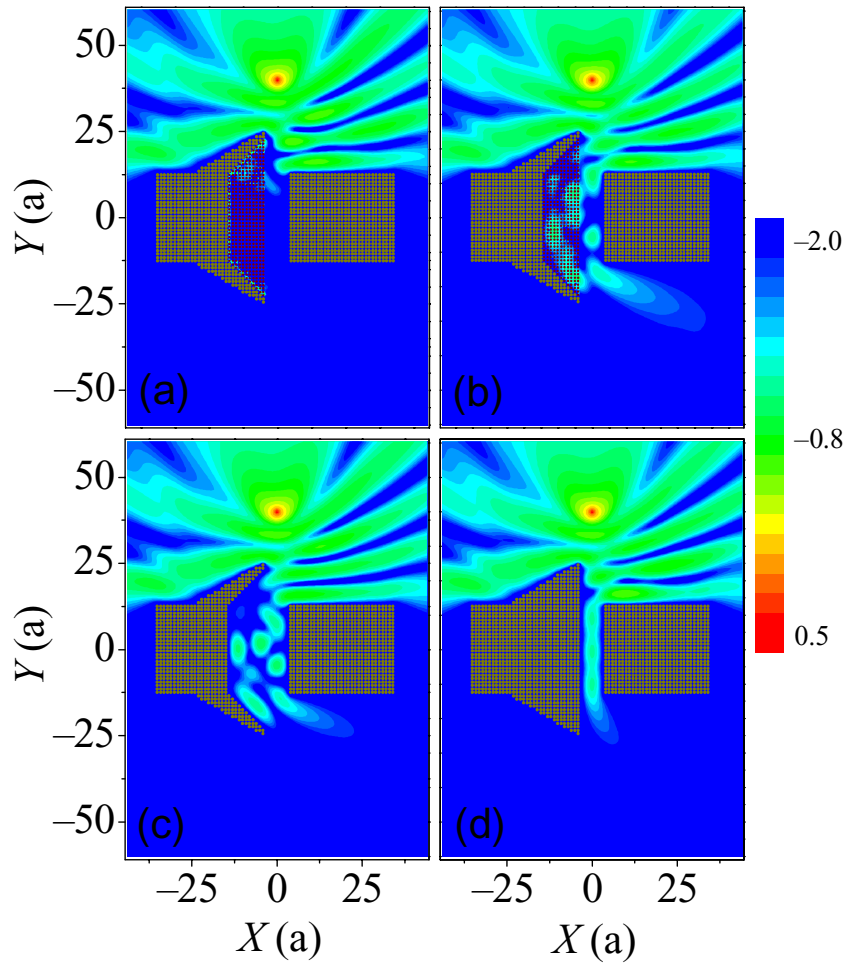


Figure 5. The implementation of the invisible gateway using magnetic photonic crystals. Here, we show the electric field intensity pattern for different geometries working at different values of the external magnetic field. (a) $H_0 = 500$ Oe, (b) $H_0 = 475$ Oe, (c) without magnetic metamaterials and (d) with magnetic metamaterial replaced by PEC.

where α_1 is the damping coefficient, $\omega_0 = \gamma_1 H_0$ is the resonance frequency with γ_1 being the gyromagnetic ratio; H_0 is the sum of the external magnetic field and shape anisotropy field along the z -direction, $\omega_m = \gamma_1 M_s$ is the characteristic frequency with M_s the saturation magnetization which is taken as $M_s = 1750$ G, typical for single-crystal yttrium–iron–garnet (YIG). As the absorption of single-crystal YIG is extremely low, we can set $\alpha_1 = 0$.

Numerical simulations of the gateway under different conditions were performed by using the multiple scattering method [30]. Figure 5 shows the electric field intensity in logarithmic scale. The bulk PEC is replaced by a discrete system of the periodically arranged PEC rods (marked with dark green solid circles in the figure), and the ferrite rods are denoted as hollow circles. Under $H_0 = 500$ Oe and the frequency $f = 2.55$ GHz, the effective refractive index of the magnetic metamaterial is $n = -1$ ($\epsilon_{\text{eff}} = \mu_{\text{eff}} = -1$). In figure 5(a), it can be seen that the electric field is excluded from the air channel, so that the open channel appears to be blocked to the eye at this frequency. This demonstrates that the gateway can be implemented by a photonic

crystal type structure in which each element (each ferrite rod in the periodic array) is identical. By changing the external field to $H_0 = 475$ Oe, the refractive index of the magnetic metamaterial becomes $n = 1$ ($\epsilon_{\text{eff}} = \mu_{\text{eff}} = 1$). The electric field intensity under such conditions is shown in figure 5(b), which shows that the channel is open for EM wave passage, or the passage appears to be open to the eye. Our results demonstrate that the gateway can be implemented by a very simple configuration and the effect is tunable by an external field. As shown in appendix A, the effect is fairly robust to the disorder of the position of ferrite cylinders. Figures 5(c) and (d) illustrate the fact that the channel is electromagnetically open if the ferrite rods are replaced by air and by PEC rods. In addition to the simple geometry and weak absorption, the magnetic metamaterial has a reasonably broad bandwidth as a DNM.

5. Conclusion

In conclusion, we showed that a robust and tunable electromagnetic gateway can be constructed using simple material parameters. The idea is conceived through consideration of transformation optics and can be realized using a photonic crystal type structure.

Acknowledgments

We thank Drs Yun Lai and Jack Ng for their helpful discussions. This work was supported by Hong Kong Central Allocation grant no. HKUST3/06C. Computation resources were supported by the Shun Hing Education and Charity Fund. SYL and ZFL were supported by CNKBRSE, NNSFC, PCSIRT and MOE of China (B06011), and Shanghai Science and Technology Commission.

Appendix A

In this appendix, we give the detailed coordinate transformation to produce the folded geometry used in the text. Let us first consider the following coordinate transformation:

$$x = \begin{cases} -x_2^y + \frac{x_2 + x_1}{x_2 - x_1} \times (x' + x_2^y), & -x_2^y < x' < -x_1^y, \\ -x', & -x_1^y < x' < 0, \\ x', & \text{else,} \end{cases} \quad (\text{A.1})$$

$$y' = y, \quad z' = z,$$

where

$$(x_1^y, x_2^y) = \begin{cases} \left(x_1 \frac{y_2 - y}{y_2 - y_1}, x_2 \frac{y_2 - y}{y_2 - y_1} \right), & y_1 < y < y_2, \\ (x_1, x_2), & -y_1 < y < y_1, \\ \left(x_1 \frac{y_2 + y}{y_2 - y_1}, x_2 \frac{y_2 + y}{y_2 - y_1} \right), & -y_2 < y < -y_1. \end{cases} \quad (\text{A.2})$$

This coordinate transformation maps the virtual space (x -space) described in figure 1(b) into the physical space (x' -space) described in figure 1(a). If the virtual space is a vacuum, we

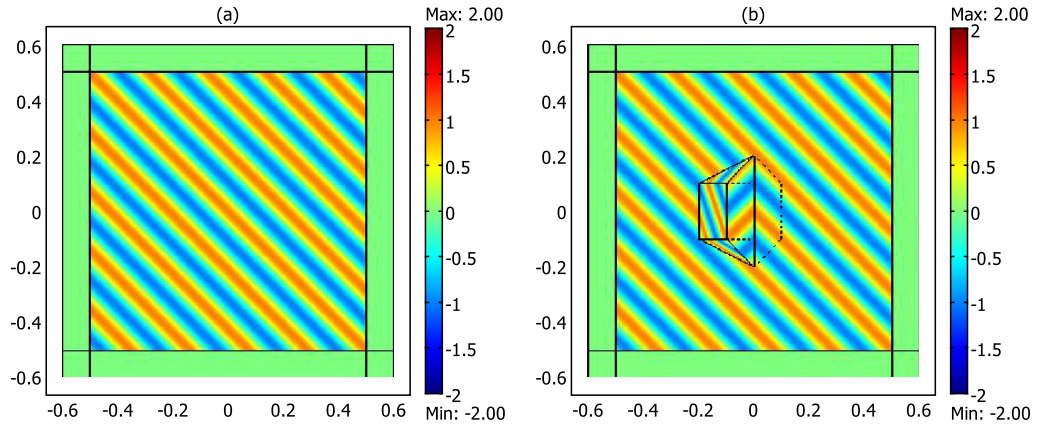


Figure A.1. The folded geometry used in the text. (a) A obliquely incident TE plane wave in free space. (b) The structure with the material described by equation (A.4) and the DNM are invisible.

can obtain the corresponding material parameters in the physical space. It contains two kinds of materials in the vacuum background, one a DNM with $\varepsilon = \mu = -1$ (shown in red in figure 1(a)), the other an anisotropic medium (shown in blue in figure 1(a)) whose parameters are derived in the following section.

We can easily obtain the Jacobian transformation matrix,

$$\Lambda = \begin{bmatrix} \frac{\partial x'}{\partial x} & \frac{\partial x'}{\partial y} & 0 \\ 0 & 1 & 0 \\ 0 & 0 & 1 \end{bmatrix} \quad (\text{A.3})$$

from equations (A.1) and (A.2) for the mapping between the blue region in figure 1(a) and the yellow region in figure 1(b), and we can also prove that $\frac{\partial x'}{\partial x} = r$ and $\frac{\partial x'}{\partial y} = p$ in the text. From transformation optics, we can obtain the material parameters for the blue region,

$$\overleftrightarrow{\varepsilon}_p = \overleftrightarrow{\mu}_p = \begin{bmatrix} \frac{r^2+p^2}{r} & \frac{p}{r} & 0 \\ \frac{p}{r} & \frac{1}{r} & 0 \\ 0 & 0 & \frac{1}{r} \end{bmatrix}. \quad (\text{A.4})$$

Figure A.1(a) shows the propagation of the incident TE polarization plane wave from the left to the right but at an angle of 45° from the x -direction in free space. The frequency is 2 GHz. We consider the object described in equation (A.4) together with a DNM domain. The scales of the structure in our simulations are the same as the ones used in the text. Figure A.1(b) shows the scattering pattern of such a structure and demonstrates that the structure itself is invisible to far-field observers.

A modification of the above-folded geometry can lead to a variety of conceptual devices. For example, if the virtual space is not a vacuum but an object of permittivity ε_s and permeability μ_s , then the parameters in the blue region should be a permittivity tensor, $\varepsilon_s \overleftrightarrow{\varepsilon}_p$, and a permeability tensor, $\mu_s \overleftrightarrow{\mu}_p$. The object in the blue region together with the DNM

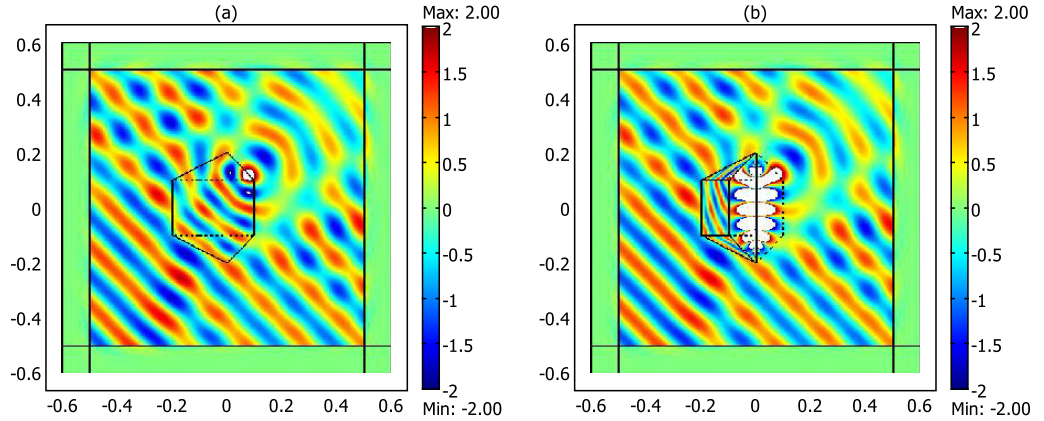


Figure A.2. The scattering pattern of an equivalent scatterer and the real scatterer. (a) The scattering pattern of an object of permittivity $\varepsilon_s = 2.25$. (b) The corresponding scattering pattern of the scattering amplifier.

domain will have a scattering cross section that can be much larger than its geometric cross section. Figure A.2(a) shows the scattering pattern of an object with permittivity $\varepsilon_s = 2.25$ and permeability $\mu_s = 1$. Figure A.2(b) shows the scattering pattern of the structure including the object with permittivity tensor $\varepsilon_s \vec{\varepsilon}_p$ and permeability tensor $\mu_s \vec{\mu}_p$ and the DNM. The two similar far-field patterns in figures A.2(a) and (b) confirm the enhanced scattering effect. In the text, we apply this structure in an inverse manner. We suppose that the object in the blue region is of permittivity ε_0 and permeability μ_0 . Then, the whole structure is equivalent to another object with permittivity and permeability tensors, $\vec{\varepsilon} = \varepsilon_0 \vec{c}$ and $\vec{\mu} = \mu_0 \vec{c}$ (described in the text). We can easily obtain equation (2) by performing an inverse transformation.

Appendix B

In this appendix, we demonstrate the robustness for the implementation of the gateway using the magnetic photonic crystal structure. We introduce disorder by displacing the ferrite rods from their original positions with

$$\Delta r = (a - 2r) \times s \times r_n, \quad (\text{B.1})$$

where a is the lattice constant, r is the radii of the ferrite rods, r_n is a uniform random variable in the interval $(-0.5, 0.5)$ (assures no overlap of cylinders), s is the strength of disorder. Figure B.1(a) corresponds to figure 5(a) but with a disorder of $s = 0.5$ introduced. The gateway remains blocked to the eye for this strength of disorder. When H_0 changes to 475 Oe, the gateway is open again as shown in figure B.1(b). Figure B.1(c) corresponds to figure 5(a) but with a strong disorder of $s = 1.0$ introduced. The functionality of the gateway is now slightly compromised but the blocking is at least partially effective at such a strength of disorder. With $H_0 = 475$ Oe, the gateway is open again as shown in figure B.1(d). The results indicate that the functionality is robust to structural perturbations.

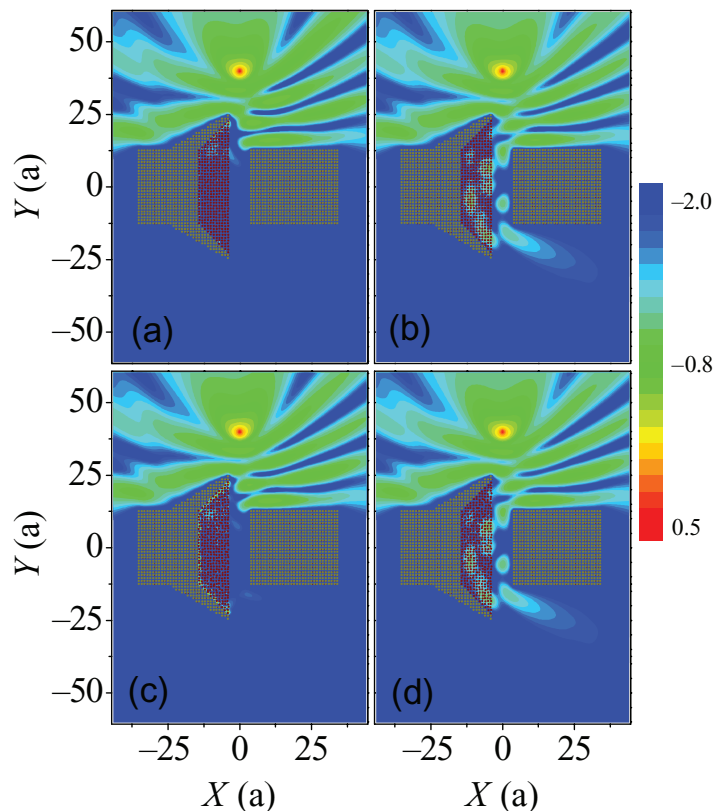


Figure B.1. The robust effect from the disorder. The electric field intensity pattern for the gateway with different levels of disorder working at different external magnetic fields. (a) $s = 0.5$, $H_0 = 500$ Oe; (b) $s = 0.5$, $H_0 = 475$ Oe; (c) $s = 1.0$, $H_0 = 500$ Oe; and (d) $s = 1.0$, $H_0 = 475$ Oe.

References

- [1] Leonhardt U 2006 *Science* **312** 1777
- [2] Pendry J B, Schurig D and Smith D R 2006 *Science* **312** 1780
- [3] Greenleaf A, Lassas M and Uhlmann G 2003 *Math. Res. Lett.* **10** 685
- [4] Schurig D, Mock J J, Justice B J, Cummer S A, Pendry J B, Starr A F and Smith D R 2006 *Science* **314** 977
- [5] Cai W, Chettiar U K, Kildishev A V and Shalaev V M 2007 *Nat. Photonics* **1** 224
- [6] Rahm M, Schurig D, Roberts D A, Cummer S A, Smith D R and Pendry J B 2008 *Photonics Nanostruct.: Fundam. Appl.* **6** 87
- [7] Chen H Y and Chan C T 2007 *Appl. Phys. Lett.* **90** 241105
- [8] Chen H Y, Hou B, Chen S, Ao X, Wen W and Chan C T 2009 *Phys. Rev. Lett.* **102** 183903
- [9] Greenleaf A, Kurylev Y, Lassas M and Uhlmann G 2007 *Phys. Rev. Lett.* **99** 183901
- [10] Kildishev A V and Narimanov E E 2007 *Opt. Lett.* **32** 3432
- [11] Zhang X, Chen H Y, Luo X and Ma H R 2008 *Opt. Express* **16** 11764
- [12] Bergamin L 2008 *Phys. Rev. A* **78** 043825
- [13] Yu G, Jiang W and Cui T J 2009 *Appl. Phys. Lett.* **94** 041904
- [14] Li J and Pendry J B 2008 *Phys. Rev. Lett.* **101** 203901
- [15] Liu R, Ji C, Mock J J, Chin J Y, Cui T J and Smith D R 2009 *Science* **323** 366

- [16] Leonhardt U and Tyc T 2009 *Science* **323** 110
- [17] Ng J, Chen H Y and Chan C T 2009 *Opt. Lett.* **34** 644
- [18] Lai Y, Chen H Y, Zhang Z Q and Chan C T 2009 *Phys. Rev. Lett.* **102** 093901
- [19] Luo X D, Yang T, Gu Y, Chen H Y and Ma H R 2009 *Appl. Phys. Lett.* **94** 223513
- [20] Rowling J R 1998 *Harry Potter and the Chamber of Secrets* (London: Bloomsbury)
- [21] Shelby R A, Smith D R and Schultz S 2001 *Science* **292** 77
- [22] Smith D R, Pendry J B and Wiltshire M C K 2004 *Science* **305** 788
- [23] Soukoulis C M, Linden S and Wegener M 2007 *Science* **315** 47
- [24] Lezec H J, Dionne J A and Atwater H A 2007 *Science* **316** 430
- [25] Yao J, Liu Z, Liu Y, Wang Y, Sun C, Bartal G, Stacy A and Zhang X 2008 *Science* **321** 930
- [26] Valentine J, Zhang S, Zentgraf T, Ulin-Avila E, Genov D A, Bartal G and Zhang X 2008 *Nature* **455** 376
- [27] Leonhardt U and Philbin T G 2006 *New J. Phys.* **8** 247
- [28] Pendry J B and Ramakrishna S A 2003 *J. Phys.: Condens. Matter* **15** 6345
- [29] Yang T, Chen H Y, Luo X D and Ma H R 2008 *Opt. Express* **16** 18545
- [30] Liu S, Chen W, Du J, Lin Z F, Chui S T and Chan C T 2008 *Phys. Rev. Lett.* **101** 157407